

Primary role of the barely occupied states in the charge density wave formation of NbSe₂

D. W. Shen^{1*}, Y. Zhang¹, L. X. Yang¹, J. Wei¹, H. W. Ou¹, J. K. Dong¹, C. He¹, B. P. Xie¹, B. Zhou¹, J. F. Zhao¹, M. Arita², K. Shimada², H. Namatame², M. Taniguchi², J. Shi³, and D.L. Feng^{1*}
¹*Department of Physics, Surface Physics Laboratory (National Key Laboratory) and Advanced Materials Laboratory, Fudan University, Shanghai 200433, P. R. China*

²*Hiroshima Synchrotron Radiation Center and Graduate School of Science, Hiroshima University, Hiroshima 739-8526, Japan and*

³*School of Physics, Wuhan University, Wuhan, 430072, P. R. China*

(Dated: March 7, 2022)

NbSe₂ is a prototypical charge-density-wave (CDW) material, whose mechanism remains mysterious so far. With angle resolved photoemission spectroscopy, we recovered the long-lost nesting condition over a large broken-honeycomb region in the Brillouin zone, which consists of six saddle band point regions with high density of states (DOS), and large regions away from Fermi surfaces with negligible DOS at the Fermi energy. We show that the major contributions to the CDW formation come from these barely occupied states rather than the saddle band points. Our findings not only resolve a long standing puzzle, but also overthrow the conventional wisdom that CDW is dominated by regions with high DOS.

2H structured niobium diselenide (NbSe₂) is one of the most studied materials for its prototypical superconductivity (SC) and two dimensional charge density wave (CDW) [1, 2, 3, 4, 5, 6]. Based on experiments conducted on NbSe₂, understanding on some of the most basic properties of SC and CDW was reached, such as the internal electronic structures of the vortex cores [7], the anisotropic s-wave [5, 6, 7] and multi-band SC [8, 9, 10, 11], the anisotropic electron-phonon interaction [6, 12], and the phonon softening at the CDW transition [13]. Nevertheless, the very mechanism of the CDW in NbSe₂ itself has been mysterious and controversial for over three decades [4, 12, 14, 15, 16], even though it is one of the very first two dimensional CDW materials discovered [17].

In a typical picture of CDW, there are usually parallel Fermi surface (FS) sections, which guarantee a large number of electrons could be scattered from one parallel side to the other by softened phonons with a fixed momentum transfer corresponding to the ordering wavevector(s). As a result, the charge susceptibility at the ordering wavevector(s) will be enhanced, and CDW instability could be induced in collaboration with lattice. This gives the so called nesting condition of CDW. Similarly, saddle band points, where the singularities of density of states (DOS) are located, were proposed to cause CDW as well [14]. Recently, the authors discussed another so-called Fermi-patch CDW mechanism for some polaronic systems, where large DOS at E_F hovers over an extended area of the Brillouin zone (BZ) and work collectively to favor certain CDW order [18]. However, the CDW in NbSe₂ cannot be explained by any of these scenarios: neither can its ordering wavevectors match the FS sections [4, 15, 16], nor match the saddle band points [15, 16], even though some experiments showed that the CDW gap does open near the saddle band points [19]; and there

are no Fermi patches. The latest experiment identified the CDW gap in the hashed circles of Fig. 4(a), some of which fulfill the nesting condition [12]. However, there are still some regions that do not. The inapplicability of these common models for CDW in such a classic compound suggests that our current understanding of CDW need to be amended.

All the existing CDW mechanisms are centered on the regions with high DOS at E_F in the BZ. In this Letter, we show that the CDW related spectral weight suppression with large energy scale occurs in a large broken-honeycomb region mainly away from the FS's, including a large momentum area where the DOS is very small at E_F . Recovery of the region makes the nesting conditions naturally fulfilled, which explains the previous controversies. Particularly, we prove that it is the states in these low-DOS regions that play a primary role in the CDW formation. Such an unexpected finding overthrows the conventional wisdom that CDW is dominated by the regions with high DOS. The electronic states in the entire BZ have to be examined no matter how low the DOS they possess.

High quality NbSe₂ single crystals were synthesized by the vapor-transport technique. The data were collected with 21.2eV photons from Helium discharge lamp and BL9 of Hiroshima synchrotron radiation center by the Scienta R4000 electron analyzers. The angular resolution is 0.3° and the total energy resolution is ~ 10 meV. In the temperature dependence studies, measurements were conducted in a cyclic way to guarantee no aging effects in the spectra. All experiments were performed in the ultra-high vacuum (better than 3×10^{-11} mbar in the helium lamp system and $\sim 5 \times 10^{-11}$ mbar at BL-9) and in a short time.

Photoemission intensity maps integrated within ± 10 meV around the Fermi energy (E_F) at the normal

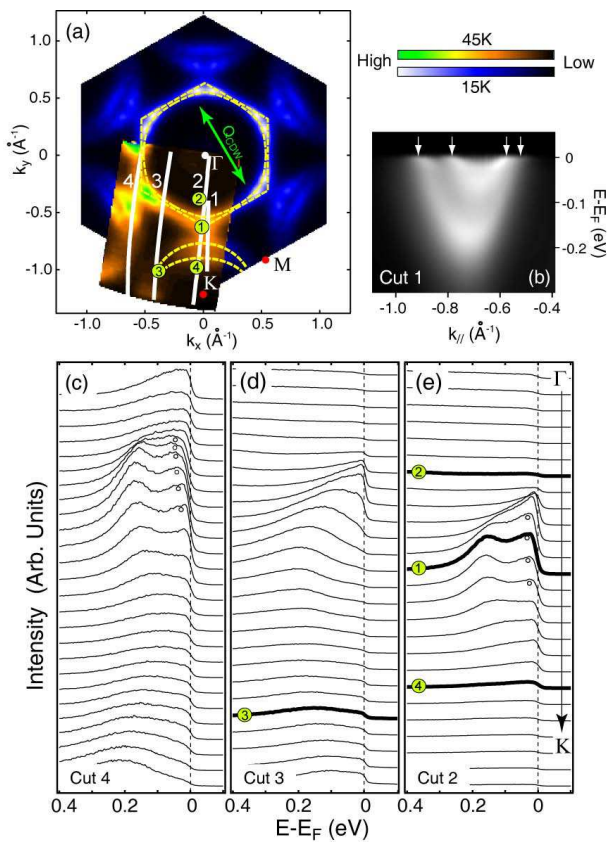


FIG. 1: (Color online) (a) Photoemission intensity maps (integrated within 20meV around E_F) at the CDW state (15K) and normal state (45K) are compared. The image taken at 15K is 6-fold symmetrized. (b) The photoemission intensity along Cut 1 marked in panel (a). (c)-(e) The typical ARPES spectra for NbSe₂ taken at normal state (45K) along the corresponding cuts. The thicker curves are the spectra at the numbered momenta in panel (a), and the open circles represent the location of the flat band.

(45K) and CDW states (15K) are compared in Fig. 1(a). Three FS pockets, one hexagon around Γ and two around \mathbf{K} point can be directly distinguished. Furthermore, because of the coupling between two NbSe₂ layers in a unit cell, two split bands can be identified [see Fig. 1(b)], which gives double-walled FS's [16, 20, 21]. Although there are long straight sections in the Γ pockets, none of them could be connected by the CDW wavevector $\mathbf{Q}_i \sim \mathbf{a}_i^*/3 = 0.688 \text{ \AA}^{-1} (i=1,2,3)$ [22].

Figs. 1(c-e) illustrate the normal state spectra of NbSe₂ along three cuts across FS's. None of them exhibits a sharp quasiparticle-like lineshape, even at the Fermi crossings. However, they do show clear dispersions, which make the FS's well defined. These have been found to be typical signatures of polaronic systems, such as La_{1.2}Sr_{1.8}Mn₂O₇ and K_{0.3}MoO₃, where the weight of the quasiparticle peak is vanishingly small, and its dispersion is renormalized to the vicinity of the FS. However, the majority of states are distributed to much higher

energies as incoherent spectral weight by scattering of multi-phonons[23, 24], which interestingly, still follows the bare band dispersion. We note that in NbSe₂ the spectral weight at E_F quickly drops when away from the FS's, unlike a sibling compound 2H-Na_xTaS₂, where large spectral weight at E_F is observed almost over the entire BZ [18]. Moreover, midway between Γ and \mathbf{K} , where the saddle band points stand, we indeed observe the flat dispersion as marked by the open circles in Figs. 1(c) and 1(e). Even though the spectral centroid is below E_F , the DOS is quite high here.

The intensity maps do not show any typical CDW effects, such as the folding of the FS's. However, through careful examination of the spectra, the suppression upon CDW is observed in various regions of the BZ. Several representative spectra are plotted in Figs. 2(a-d) for illustration. The corresponding momenta are marked in Fig. 1(a) and their corresponding spectra have been highlighted in Figs. 1(d-e). The left panel of Fig. 2(a) shows a spectral lineshape evolution as a function of temperature near the saddle band point. The spectra taken at 45K and 35K, which are both above the CDW transition temperature 33K, nearly coincide with each. Once entering the CDW state, the spectrum is suppressed noticeably over about 80 meV below E_F while the leading edge shifts negligibly. This suppression energy scale is much higher than the $k_B T_c$ of 3 meV, which is the energy scale of CDW effects on the quasiparticles. Such low energy effects might be passed to the incoherent spectral weight at high energies by multi-phonon scattering processes as observed here.

The suppression at saddle point agrees with previous observations [12]. However, the main discovery here is that such CDW related suppression also occurs over large momentum regions inside the Γ pocket [Fig. 2(b)] and around the M point [Fig. 2(c)], though the spectral weights at E_F are low there [see Figs. 1(d-e)]. Whereas, for the spectra taken inside the \mathbf{K} pocket [Fig. 2(d)], no such suppression is observed. To show the suppression is not due to thermal broadening, all spectra are divided by the resolution convoluted Fermi functions at corresponding temperatures and then multiplied by that of 10K, before they are compared in the right panels of Figs. 2(a-d). While the suppression at momenta No.1-3 is observed upon CDW formation, it is absent at momentum No.4. This is further illustrated by the spectral weight suppression ratios in Fig. 2(e). We stress that such subtle spectral weight suppression is assured to be purely dependent of temperature instead of the aging effects or noises. Besides the high sampling points and fine statistic, at the end of the temperature evolution study, the first spectrum is always repeated to make sure they overlap, as testified by the two coincident 15K spectra in Fig. 2(a).

Following this analysis, more than 1,200 pairs of the normal and CDW state spectra were compared one by

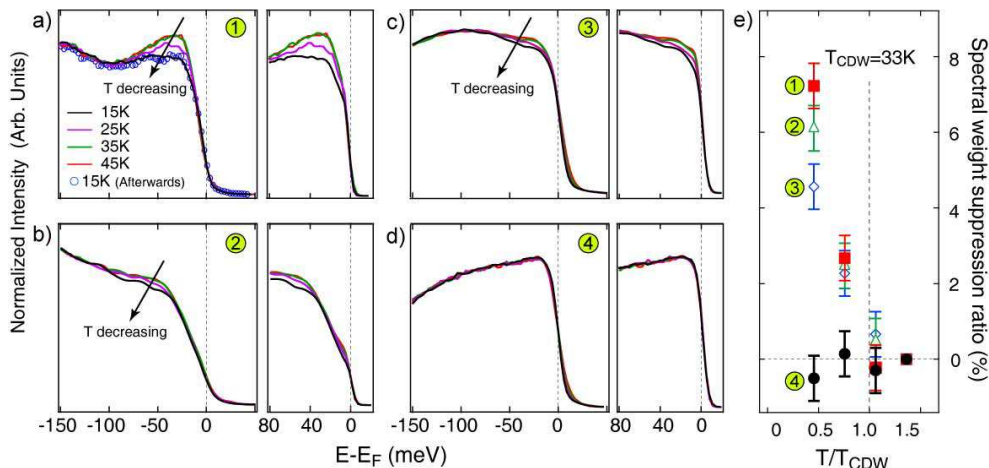


FIG. 2: (Color online) (a)-(d) Typical temperature dependence of the original (left) and temperature broadening effects removed (right) spectra in the normal and CDW states at momenta No.1-4 marked in Fig. 1(a) respectively (see text for details). (e) The spectral weight suppression ratios (compared to spectra taken at 45K and over (E_F-80 meV, E_F)) for different temperatures in fig (a-d) respectively.

one over more than 1/6 of the BZ. Figs. 3(c-h) give some more examples, where the left panels show the raw spectra, and right panels show the corresponding spectra with thermal broadening removed as practised in Fig. 2. Eventually, the momenta regions where the spectral weight is suppressed can be determined accurately, as marked in Fig. 3(a) by bars. These regions are mainly composed of the large domains inside the Γ pockets, around the \mathbf{M} points, and around the saddle band points. Such distribution has been confirmed by many samples, and the results based on two of them are shown here. Note this distribution includes some “barely occupied” regions where the DOS at E_F is very weak. We emphasize that the weak spectral weight and its suppression are not due to the umklapp scattering of the CDW order, since it is not observed in the FS or dispersion.

To further visualize the distribution of the weight suppression, the intensity map at 15K [integrated over (E_F-80 meV, E_F)] is subtracted from that at 45K, and the result is shown in the upper half of Fig. 3(b). Note the thermal broadening effects have been removed from the spectra following the standard symmetrization method before the processing [25]. After normalized by the intensity map at 45K, the resulting spectral weight suppression ratio map [lower part of Fig. 3(b)] further highlights the weight-suppressed regions, which are consistent with those determined in Fig. 3(a). Note we have surveyed the entire BZ, and only observed suppression instead of spectral weight gain in the measured energy range. Considering the conservation of the total electrons, the suppressed weight should be shifted to some higher binding energies. In this way, the electronic energy gain for the CDW transition is naturally fulfilled.

The distribution of the CDW induced spectral weight suppression makes a broken-honeycomb-shaped structure

in the BZ, as shown by Fig. 4(a). The suppression over the saddle band regions (surrounded by the dotted lines) only account for 43% of the total one. In other words, although the DOS is higher around the saddle band points, it only plays a secondary role in the CDW formation due to its relatively small momentum space. Moreover, the broken-honeycomb regions can be well connected by the CDW wavevector \mathbf{Q}_i 's [represented by the double-headed arrows in Fig. 4(a)]. In previous studies, since only a small portion of the weight-suppressed region was discovered (hashed circles), multiple scattering has to be invoked to barely make some of the regions connected by the two dashed arrows in Fig. 4(a) [12]. However, this multiple scattering assumption is not needed, once the large weight-suppressed region is recovered here.

To further demonstrate the contribution to the CDW instability of the broken-honeycomb-shaped region, we calculated the weighted joint DOS,

$$C(\vec{q}, \omega) \equiv \int M(\vec{k}, \vec{k} + \vec{q}) A(\vec{k}, \omega) A(\vec{k} + \vec{q}, \omega) d\vec{k}$$

, where $M = \begin{cases} 1 & (\vec{k} + \vec{q}, \vec{k} \in \text{gapped region}) \\ 0 & (\text{otherwise}) \end{cases}$. It has

been shown before that $C(\vec{q}, 0)$ could effectively describe the phase space for scattering of electrons from the state at \vec{k} to the state at $\vec{k} + \vec{q}$ by certain modes with wavevector \vec{q} , and it is closely associated with the electronic susceptibility [18, 26, 27]. The matrix element $M(\vec{k}, \vec{k} + \vec{q})$ is introduced assuming that only the states that directly couple (thus suppressed) with the softening phonon branch around \mathbf{Q}_i [13], would contribute to the CDW instability. $C(\vec{q}, 0)$'s computed on the honeycomb regions [Fig. 4(b)] and on the saddle band regions [Fig. 4(c)] are plotted in the same scale. Clearly, the peaks at \mathbf{Q}_i 's are very prominent in Fig. 4(b), whereas they are not so pronounced in

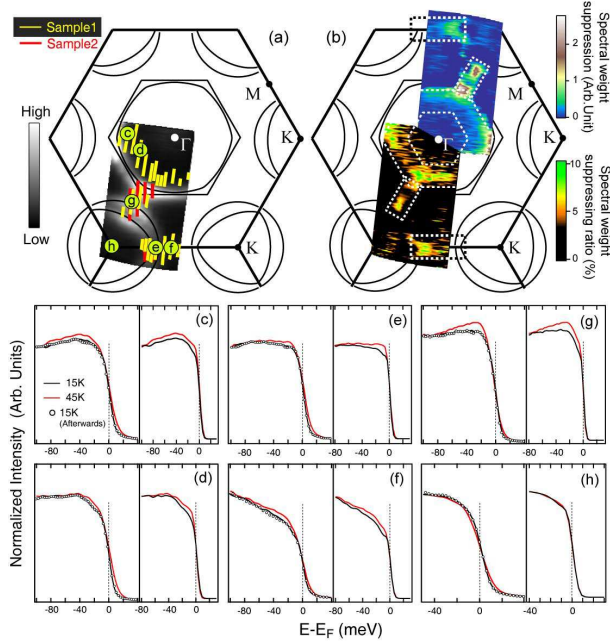


FIG. 3: (Color online) (a) The illustration of the regions where gap opening occurs upon CDW transition in the first BZ. The gapped regions determined by comparison of the spectra below and above T_{CDW} one by one. (b) The spectral weight suppression map and its corresponding ratio map (see text for detail) are false color plotted, where the dashed lines contour the obviously suppressed regions and the black ones indicate the FS's. (c)-(h) Typical spectra (left) and the corresponding thermal broadening removed ones (right) in the normal and CDW states at momenta marked in panel (a).

Fig. 4(c). This is more clearly illustrated in Fig. 4(d), where the $C(q, 0)$'s along the Γ -M direction are compared. The saddle band regions only contribute about 17% of the total $C(Q_i, 0)$ computed over the broken-honeycomb region respectively [28]. Therefore, the nesting of states with low DOS at E_F indeed dominates the charge instability at Q_i 's here.

The data here also provide some clues on the driving force behind the unconventional CDW transition in NbSe₂. For the conventional Peierls transition at one dimension, the CDW is driven by the electronic energy gain, and it is reflected by a peak in the charge susceptibility [29]. Although it might be more complicated in NbSe₂, the observed peak in the weighted joint DOS does hint that the electronic energy gain might be the dominating factor here as well.

In conclusion, we have found that the CDW related spectral weight suppression in the large broken-honeycomb region mainly away from the FS's for NbSe₂, which naturally fulfills the nesting condition, and resolves a long-standing puzzle of this classic CDW material. Despite of the weak DOS in most of this region, their primary role in the CDW formation is demonstrated. Our findings show that collective contribution of the weakly

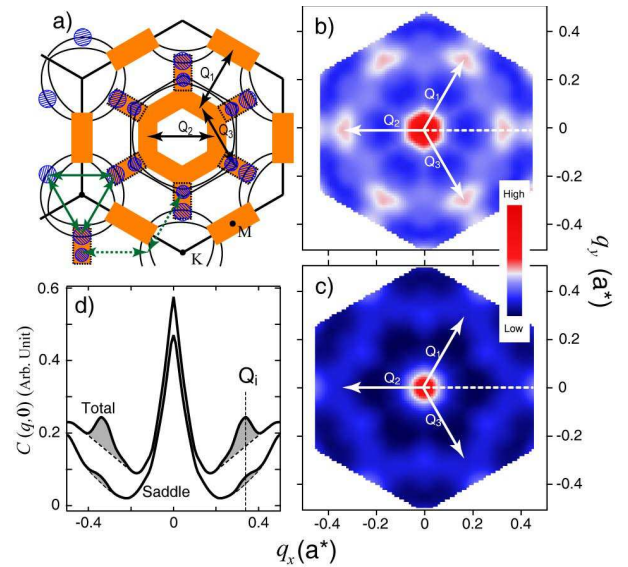


FIG. 4: (Color online) (a) The distribution of CDW related weight suppression over the entire BZ sketched from the spectral weight suppression map, which are marked by the orange broken-honeycomb-shaped structure. The gapped regions could be well connected by the CDW wavevectors, Q_i 's ($i=1,2,3$), as indicated by the double-headed arrows. The gapped regions proposed by Kiss *et al.* and around the saddle band points are marked by the hashed circles and the dotted line surrounded rectangles. (b)-(c) Two dimensional joint DOS results on the honeycomb regions and the saddle band point regions, respectively. (d) Comparison of the corresponding joint DOS results along the dashed lines in panels (b) and (c).

occupied states can play the primary role in CDW formation in some cases, and thus should not be overlooked, which amends the conventional wisdom of CDW.

We gratefully acknowledge the helpful discussion with Profs. Q. H. Wang, T. Xiang, J. X. Li, and H. Q. Lin. This work was supported by NSFC, MOST (973 project No.2006CB601002 and No.2006CB921300), and STCSM of China.

* Electronic address: dwshen@fudan.edu.cn; dlifeng@fudan.edu.cn

- [1] As documented in <http://apps.isiknowledge.com/>, there have been nearly 800 papers published solely on NbSe₂ so far.
- [2] E. Revolinski, B. E. Brown, D. Beerntsen, and C. H. Armitage, *J. Less-Common Met.* **8**, 63 (1965).
- [3] J. M. E. Harper, T. H. Geballe, and F. J. DiSalvo, *Phys. Lett.* **54A**, 27 (1975).
- [4] Th. Straub *et al.*, *Phys. Rev. Lett.* **82**, 4504 (1999).
- [5] T. Yokoya *et al.*, *Science* **294**, 2518 (2001).
- [6] T. Valla *et al.*, *Phys. Rev. Lett.* **92**, 086401 (2004).
- [7] H. J. Choi *et al.*, *Nature (London)* **418**, 758 (2002).
- [8] J. E. Sonier, M. F. Hundley, J. D. Thompson, J. W. Brill, *Phys. Rev. Lett.* **82**, 4914 (1999).

- [9] E. Boaknin *et al.*, Phys. Rev. Lett. **90**, 117003 (2003).
- [10] J. D. Fletcher *et al.*, Phys. Rev. Lett. **98**, 057003 (2007).
- [11] V. Barzykin and L. P. Gorkov, Phys. Rev. Lett. **98**, 087004 (2007).
- [12] T. Kiss *et al.*, Nature Physics **3**, 720 (2007).
- [13] D. E. Moncton, J. D. Axe and F. J. Di Salvo, Phys. Rev. B **16**, 801 (1977).
- [14] T. M. Rice and G. K. Scott, Phys. Rev. Lett. **35**, 120 (1975).
- [15] K. Rossnagel *et al.*, Phys. Rev. B **64**, 235119 (2001).
- [16] M. D. Johannes, I. I. Mazin and C. A. Howells, Phys. Rev. B **73**, 205102 (2006).
- [17] J. A. Wilson, F. J. Di Salvo and S. Mahajan, Adv. Phys. **24**, 117 (1975).
- [18] D. W. Shen *et al.*, Phys. Rev. Lett. **99**, 216404 (2007).
- [19] W. C. Tonjes, V. A. Greanya, R. Liu, C. G. Olson, P. Molinie, Phys. Rev. B **63**, 235101 (2001).
- [20] L. F. Mattheiss, Phys. Rev. B **8**, 3719 (1973).
- [21] R. Corcoran, J. phys. Condens. Matter **6**, 4479 (1994).
- [22] D. E. Moncton, J. D. Axe and F. J. Di Salvo, Phys. Rev. Lett. **34**, 734 (1974).
- [23] N. Mannella *et al.*, Nature (London) **438**, 474 (2005).
- [24] José-Luis Mozos, Pablo Ordejón and Enric Canadell, Phys. Rev. B **65**, 233105 (2002).
- [25] M. R. Norman *et al.*, Nature (London) **392**, 157 (1998).
- [26] U. Chatterjee *et al.*, Phys. Rev. Lett. **96**, 107006 (2006).
- [27] K. McElroy *et al.*, Phys. Rev. Lett. **96**, 067005 (2006).
- [28] Alternatively, if estimated based on the height, the ratio is about 28%.
- [29] G. Grüner, *Density Waves in Solids*. (Addison-Wesley Longman, **1994**)